On preference of Yoshida construction over Forest–Ruth fourth-order symplectic algorithm

Article *in* The European Physical Journal C · May 2013

DOI: 10.1140/epjc/s10052-013-2413-y

3 authors, including:

Lijie Mei
Yunnan Normal University
30 PUBLICATIONS **462** CITATIONS

SEE PROFILE

Xin Wu
Nanchang University
118 PUBLICATIONS **2,547** CITATIONS

SEE PROFILE

Eur. Phys. J. C (2013) 73:2413
DOI 10.1140/epjc/s10052-013-2413-y

THE EUROPEAN PHYSICAL JOURNAL C

Regular Article - Theoretical Physics

On preference of Yoshida construction over Forest–Ruth fourth-order symplectic algorithm

Lijie Mei[1], **Xin Wu**[1,2,a], **Fuyao Liu**[3]

[1]School of Science, Nanchang University, Nanchang 330031, China
[2]Purple Mountain Observatory, Chinese Academy of Sciences, Nanjing 210008, China
[3]School of Mathematics and Information, Shanghai Lixin University of Commerce, Shanghai 201600, China

Received: 10 December 2012 / Revised: 26 March 2013 / Published online: 8 May 2013

Abstract The Forest–Ruth fourth-order symplectic algorithm is identical to the Yoshida triplet construction when all component integrators of both algorithms are exactly known. However, this equality no longer holds in general when some or all of the components are inexact and when they are second-order with odd-order error structures. The former algorithm is only second-order accurate in most cases, whereas the latter can be fourth-order accurate. These analytical results are supported by numerical simulations of partially separable but globally inseparable Hamiltonian systems, such as the post-Newtonian Hamiltonian formulation of spinless compact binaries. Therefore, the Yoshida construction has intrinsic merit over the concatenated Forest–Ruth algorithm when inexact component integrators are used.

1 Introduction

Highly efficient numerical integrators with good long-term behavior should be used to describe properly the qualitative dynamical properties of complicated systems. Geometric integration algorithms can satisfy this requirement [1]; for instance, manifold correction schemes [2, 3] that are used for forcing numerical paths to return to their real hypersurfaces given by integrals of motion, symmetric methods [4] and symplectic integrators [1, 5, 6] for Hamiltonian canonical equations of motion. In particular, the symplectic integrators are the optimum numerical tools for the qualitative investigation of the long-time evolution of Hamiltonian systems in the solar system dynamics because these integrators preserve the symplectic structure of the phase space and do not result in secular changes when creating an error in the energy integral.

Symplectic methods can be categorized into explicit or implicit types. Explicit symplectic methods are used in a Hamiltonian systems that can be divided into integrable parts. The second-order leapfrog method, the Forest–Ruth fourth-order method [7] and the Yoshida fourth-order method [8] are typical examples of explicit symplectic methods. Note that all the components of the above methods are exactly known. In addition, the Yoshida algorithm is composed of the three second-order leapfrog methods, and is completely equivalent to the Forest–Ruth method. To improve significantly the numerical accuracy of an integrator for solving a system with integrable separable forms (namely a main unperturbed part and a small perturbation part), the parameter of the small perturbation, equating with the difference between the two parts, should be appear in truncation errors [9]. Along this idea, the pseudo-high-order symplectic schemes proposed in [10, 11] have good numerical performance. The implicit symplectic algorithms should be selected when systems such as a full general relativistic gravitational system have no separable forms of position and momentum variables. The Euler-centered scheme is often used because it is the simplest one of the implicitly canonical symplectic difference schemes with even-order accuracies [6].

A mixed symplectic method, which is a mixture of the explicit and implicit methods, is designed for the Hamiltonian system with an unperturbed part and an inseparable perturbation part. This type of mixed method improves the numerical accuracy and fast convergence of iteration. Therefore, it is preferred over the same implicit scheme, which acts on the whole inseparable Hamiltonian system. The details of the construction of the mixed method are given as follows. The perturbation part is integrated numerically with the second-order implicit midpoint rule [6], and the unperturbed part is solved analytically or integrated numerically with the second-order explicit leapfrog symplectic integrator. Similar to the explicit symplectic method, the

[a] e-mail: xwu@ncu.edu.cn

mixed method can be obtained easily by using a symmetric composition of the analytical/explicit solutions and the implicit numerical solutions. An example of the second-order mixed symplectic integrator is given in the article of Liao [12]. Preto and Saha [13] developed Liao's integrator and integrated adaptive time steps to calculate post-Newtonian (*PN*) orbits of the Galactic-center stars. Recently, Lubich et al. [14] presented a fourth-order non-canonically mixed symplectic integration scheme of Suzuki [15] to solve numerically the *PN* motion of a spinning black-hole binary. More recently, Zhong et al. [16] utilized the canonical spin variables [17] to design canonically mixed symplectic integrators, involving the Forest–Ruth [7] and the optimized Forest–Ruth-like versions [18] of the *PN* Hamiltonian system of spinning compact binaries [19].

Note that the explicit or implicit component integrators in the symmetric composite formulas of a mixed method are approximate. In this case, whether both Forest–Ruth fourth-order mixed symplectic and Yoshida algorithms are still of fourth-order accuracy remains a question. Therefore,we should determine whether both algorithms have equivalent numerical performance. This issue will be addressed in this paper.

The rest of this paper is organized as follows. In Sect. 2, an analysis of the quality of the Forest–Ruth mixed symplectic and Yoshida algorithms is given in detail. Section 3 checks the performance of the two mixed methods by conducting numerical simulations of partially separable but globally inseparable Hamiltonian systems, e.g., the *PN* Hamiltonian formulation of spinless compact binaries [19]. Finally, Sect. 4 concludes the paper.

2 Performance analysis of mixed symplectic algorithms

An n-dimensional Hamiltonian system $H(\boldsymbol{p},\boldsymbol{q})$ is supposed to have the splitting form

$$H(\boldsymbol{p},\boldsymbol{q}) = H_1(\boldsymbol{p},\boldsymbol{q}) + H_2(\boldsymbol{p},\boldsymbol{q}), \tag{1}$$

where H_1 is a separable variable form of momenta $\mathbf{p}$ and positions $\mathbf{q}$,

$$H_1(\boldsymbol{p},\boldsymbol{q}) = T(\mathbf{p}) + V(\mathbf{q}), \tag{2}$$

but $H_2(\boldsymbol{p},\boldsymbol{q})$ is not. If H_1 is integrable, then an exact analytical solution exists in principle. Here, $A(\tau)$ is used to denote an operator for solving H_1,

$$A(\tau) = \exp(\tau \tilde{H}_1), \tag{3}$$

where τ denotes a time step, and $\tilde{H}_1$ is a Lie derivative with respect to H_1:

$$\tilde{H}_1 = \{\cdot, H_1\} = \frac{\partial H_1}{\partial \boldsymbol{p}}\frac{\partial}{\partial \boldsymbol{q}} - \frac{\partial H_1}{\partial \boldsymbol{q}}\frac{\partial}{\partial \boldsymbol{p}}.$$

Additionally, $A(\tau)$ can always be computed approximately by the second-order explicit leapfrog symplectic integrator

$$A(\tau) = \exp\left(\frac{\tau}{2}\tilde{T}\right)\exp(\tau\tilde{V})\exp\left(\frac{\tau}{2}\tilde{T}\right) + X\tau^3 + Y\tau^5 + \cdots. \tag{4}$$

Note that $\tilde{T}$ and $\tilde{V}$ are, respectively, the Lie derivatives of T and V, and X and Y are the complicated commutators of $\tilde{T}$ and $\tilde{V}$. Let $B(\tau)$ represent an operator of H_2. In most cases, neither analytical solution nor explicit numerical solution is present for H_2. However, $B(\tau)$ can be given approximately by the second-order implicit midpoint rule $S_{imr}(\tau)$ [6]:

$$B(\tau) = S_{imr}(\tau) + X'\tau^3 + Y'\tau^5 + \cdots, \tag{5}$$

where X' and Y' are operators associated with the high-order derivatives of H_2. Let us consider the construction of mixed symplectic integrators on the basis of the symmetric compositions of the exact component integrator $A(\tau)$ by Eq. (3) (or the inexact integrator $A(\tau)$ by Eq. (4)) and the inexact integrator $B(\tau)$ by Eq. (5).

Similar to second-order explicit symplectic methods, second-order mixed symplectic algorithms have two expressional forms

$$S_2(\tau) = A\left(\frac{\tau}{2}\right)B(\tau)A\left(\frac{\tau}{2}\right) + C\tau^3 + D\tau^5 + \cdots, \tag{6}$$

$$S_2^*(\tau) = B\left(\frac{\tau}{2}\right)A(\tau)B\left(\frac{\tau}{2}\right) + C^*\tau^3 + D^*\tau^5 + \cdots, \tag{7}$$

where C, D, C^* and D^* are complicated commutators of A and B. The above expressions can be found in Refs. [12, 13, 20]. Equations (6) and (7) can be used to construct the Forest–Ruth and Yoshida algorithms. The details of the construction are listed below.

$A(\tau)$ is initially assumed as the exact operator (3). On the basis of Eq. (6), we can derive that the triple product of S_2,

$$S_4(\tau) = S_2(\lambda\tau)S_2\big((1-2\lambda)\tau\big)S_2(\lambda\tau), \tag{8}$$

has the sum of all the third-order errors of S_2, $\bar{C}C\tau^3$, where $\bar{C}$ is a coefficient of the form

$$\bar{C} = 2\lambda^3 + (1-2\lambda)^3. \tag{9}$$

If $\bar{C} = 0$, then we have

$$\lambda = \frac{1}{2 - 2^{1/3}}. \tag{10}$$

The above equation denotes that the third-order errors of $S_2(\tau)$ have vanished. When $B(\tau)$ is exact, Eq. (8) with Eq. (10) is the Yoshida fourth-order symplectic integrator [8]. However, if $B(\tau)$ is computed approximately by

Eq. (5), the sum of all the third-order errors of $B(\tau)$ remains zero because the sum contains the factor $\bar{C}$. This situation is evident because both $B(\tau)$ and $S_2(\tau)$ have the same time coefficients. Therefore, the Yoshida construction (8) is fourth-order with an error structure of the form $(\bar{D}\tau^5 + \bar{E}\tau^7 + \cdots)$. By concatenating the edge factors of $A(\tau)$ between the right S_2 and the middle S_2 of Eq. (8),

$$A\left(\frac{1-2\lambda}{2}\tau\right)A\left(\frac{\lambda}{2}\tau\right) = A\left(\frac{1-\lambda}{2}\tau\right), \tag{11}$$

and those between the middle S_2 and the left S_2,

$$A\left(\frac{\lambda}{2}\tau\right)A\left(\frac{1-2\lambda}{2}\tau\right) = A\left(\frac{1-\lambda}{2}\tau\right), \tag{12}$$

we can obtain the Forest–Ruth algorithm [7]

$$FR(\tau) = A\left(\frac{\lambda}{2}\tau\right)B(\lambda\tau)A\left(\frac{1-\lambda}{2}\tau\right)B\big((1-2\lambda)\tau\big) \times A\left(\frac{1-\lambda}{2}\tau\right)B(\lambda\tau)A\left(\frac{\lambda}{2}\tau\right). \tag{13}$$

The inexact $B(\tau)$ is unaffected in these concatenations, so the FR algorithm should remain the same accuracy of the Yoshida method S_4, too.

Let us consider the numerical performance of these algorithms when the exact $A(\tau)$ and the inexact $B(\tau)$ are exchanged in Eq. (6); i.e., $S_2(\tau)$ is replaced with $S_2^*(\tau)$. In this case, the Yoshida construction becomes

$$S_4^*(\tau) = S_2^*(\lambda\tau)S_2^*\big((1-2\lambda)\tau\big)S_2^*(\lambda\tau). \tag{14}$$

Considering that λ is still given by Eq. (10), the third-order errors $(\bar{C}^*C^*\tau^3)$ of $S_2^*(\tau)$, as well as those of B, are eliminated naturally because the coefficient $\bar{C}^*$ is identical to zero,

$$\bar{C}^* = 4\left(\frac{\lambda}{2}\right)^3 + 2\left(\frac{1-2\lambda}{2}\right)^3 = \frac{1}{4}\big[2\lambda^3 + (1-2\lambda)^3\big] = 0. \tag{15}$$

The above equation denotes that the Yoshida method S_4^* is still fourth-order. However, if the edge factors of B in S_4^* are concatenated, i.e., A in Eqs. (11) and (12) gives place to B, then the Forest–Ruth algorithm

$$FR^*(\tau) = B\left(\frac{\lambda}{2}\tau\right)A(\lambda\tau)B\left(\frac{1-\lambda}{2}\tau\right)A\big((1-2\lambda)\tau\big) \times B\left(\frac{1-\lambda}{2}\tau\right)A(\lambda\tau)B\left(\frac{\lambda}{2}\tau\right) \tag{16}$$

is only second-order because there are non-vanishing third-order errors of B, $\tilde{C}^*C^*\tau^3$, where

$$\tilde{C}^* = 2\left(\frac{\lambda}{2}\right)^3 + 2\left(\frac{1-2\lambda}{2}\right)^3 = \frac{1}{4}\big[\lambda^3 + (1-2\lambda)^3\big] \neq 0. \tag{17}$$

However, if $A(\tau)$ of the above-mentioned algorithms is the inexact operator (4), then the conditions $\bar{C} = 0$ and $\bar{C}^* = 0$ can guarantee that the Yoshida constructions S_4 and S_4^* will reach fourth-order accuracy. In addition, Eq. (17) shows explicitly that the Forest–Ruth methods FR and FR^* only have two orders of magnitude.

The above analysis shows that the Yoshida constructions are greatly superior to the Forest–Ruth algorithms when the inexact component integrators are used. The following points are also worth noting. (i) If H_2 is a separable variable form, then H_2 can be solved numerically by the second-order explicit leapfrog integrator. Therefore, B is inexact and has second-order accuracy with a similar odd-order error structure as that of (4). In this sense, the above analytical results still hold. (ii) Only when A and B have either the odd-order error structures of (4) and (5) or have at least fourth-order accuracy can the Yoshida constructions be fourth-order. Otherwise, the Yoshida constructions will no longer be fourth-order. If A is approximately obtained from a second-order non-symmetric symplectic (or non-symplectic) algorithm A_2 and has the following error structure:

$$A(\tau) = A_2 + \breve{C}\tau^3 + \breve{D}\tau^4 + \cdots, \tag{18}$$

then the Yoshida constructions would have three orders of magnitude. (iii) If both A and B have at least fourth-order accuracy, then the Forest–Ruth algorithms would become fourth-order. (iv) The above idea can be extended to higher orders. The triple product of S_4,

$$S_6(\tau) = S_4(\lambda\tau)S_4\big((1-2\lambda)\tau\big)S_4(\lambda\tau), \tag{19}$$

removes the fifth-order errors of S_4 when

$$2\lambda^5 + (1-2\lambda)^5 = 0, \quad \text{i.e., } \lambda = \frac{1}{2-2^{1/5}}. \tag{20}$$

By repeating the above procedures, we would obtain the Yoshida sixth-order constructions and the concatenated Forest–Ruth fourth-order algorithms if A and B have fourth-order accuracy with odd-order errors. Similar demonstrations are also suitable for the eighth, tenth etc. orders.

3 Numerical checks

To check further the reliability of the above analytical results, we choose two inseparable variable Hamiltonian sys-

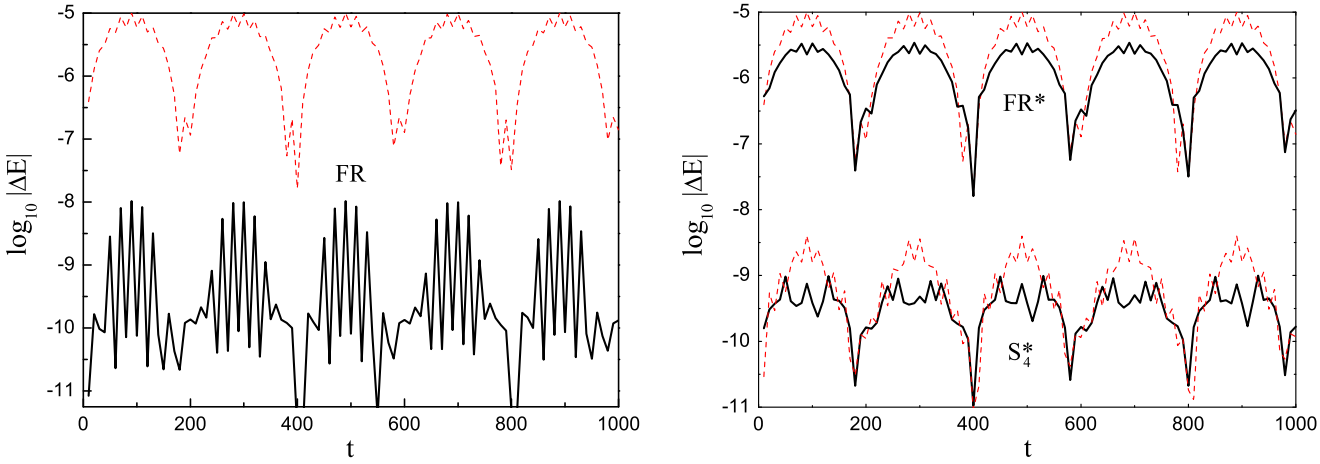

Fig. 1 Energy errors of both Forest–Ruth methods *FR* and *FR** and the Yoshida scheme S_4^* acting on a system (22). The *solid lines* deal with the case in which the H_1 part is solved analytically by Eq. (3), whereas the *dash lines* correspond to the case in which the H_1 part is solved numerically by Eq. (4) (Color figure online)

tems, and evaluate the practical numerical performance of the Forest–Ruth and Yoshida mixed symplectic algorithms. All numerical experiments in this paper are performed in a double precision environment, in which the iteration precision is in the magnitude of 10^{-14}.

3.1 A simple inseparable variable system

Let us take a simple inseparable variable system

$$H(p,q) = H_1(p,q) + H_2(p,q), \tag{21}$$

as an example, where the two parts of the system are

$$\begin{aligned} H_1(p,q) &= \frac{1}{2}\left(p^2+q^2\right), \\ H_2(p,q) &= \cos p \sin q. \end{aligned} \tag{22}$$

The operator A is exact by analytically solving H_1. A is inexact if the second-order explicit integrator (4) is used to integrate numerically H_1. However, the operator B on H_2 is given inexactly by the second-order implicit midpoint rule (5).

Given the initial conditions $(p(0), q(0)) = (1, 0)$ and the time step $\tau = 0.01$, the energy errors of the mixed integrators are shown in Fig. 1. If A is exact such as in Eq. (3), then the error of the *FR* algorithm or the Yoshida method S_4^* is smaller by three to four orders of magnitude than that of the *FR** algorithm. However, if A is similar to Eq. (4) and inexact, then *FR* has almost the same accuracy as that of *FR**. The accuracy of the algorithms S_4^* and *FR** becomes slightly better when using an exact A compared with using an inexact A. Therefore, the error from the numerical solution of H_1 exerts some influence on global numerical integration errors. However, this influence is not large enough. The error of the Yoshida method S_4 is not plotted because the error is almost the same as that of the algorithm S_4^* whether A is exact or not.

Simulations of the simple model (22) show that the Forest–Ruth and Yoshida algorithms are explicitly correct to complete different orders in most cases. The following numerical test shows the performance of these algorithms when a more complicated model is considered.

3.2 Post-Newtonian Hamiltonian of compact binaries

For two compact bodies with masses m_1 and m_2 ($m_1 \le m_2$), we take the total mass $M = m_1 + m_2$ and the reduced mass $\mu = m_1 m_2/M$. The mass ratio $\gamma = m_1/m_2$, $\eta = \mu/M = \gamma/(1+\gamma)^2$ and geometric units $c = G = 1$ are used. In the center-of-mass frame, $\boldsymbol{p}$ and $\boldsymbol{q}$, respectively, denote the momenta of body 1 relative to the center and the position coordinates of body 1 relative to body 2, where the momenta are measured in terms of μ, and the distances are measured in terms of M. The unit vector is $\boldsymbol{n} = \boldsymbol{q}/q$ with $q = |\boldsymbol{q}|$.

By using these parameters and state variables, we can express a conservative non-spin compact binary system in the *PN* Hamiltonian formulation [19]

$$H = H_N + H_{PN}. \tag{23}$$

The Newtonian term is the Kepler flow

$$H_N = \frac{\boldsymbol{p}^2}{2} - \frac{1}{q}. \tag{24}$$

The orbital *PN* terms include the 1*PN*, 2*PN* and 3*PN* order terms, namely,

$$H_{PN} = H_{1PN} + H_{2PN} + H_{3PN}. \tag{25}$$

The orbital *PN* terms are expressed as

$$H_{1PN} = \frac{1}{8}(3\eta - 1)\big(\boldsymbol{p}^2\big)^2 - \frac{1}{2}\big[(3+\eta)\boldsymbol{p}^2 + \eta(\boldsymbol{n}\cdot\boldsymbol{p})^2\big]\frac{1}{q} + \frac{1}{2q^2}, \tag{26}$$

$$\begin{aligned} H_{2PN} = {} & \frac{1}{16}\big(1 - 5\eta + 5\eta^2\big)\big(\boldsymbol{p}^2\big)^3 \\ & + \frac{1}{8}\big[\big(5 - 20\eta - 3\eta^2\big)\big(\boldsymbol{p}^2\big)^2 \\ & - 2\eta^2(\boldsymbol{n}\cdot\boldsymbol{p})^2\boldsymbol{p}^2 - 3\eta^2(\boldsymbol{n}\cdot\boldsymbol{p})^4\big]\frac{1}{q} + \frac{1}{2}\big[(5+8\eta)\boldsymbol{p}^2 \\ & + 3\eta(\boldsymbol{n}\cdot\boldsymbol{p})^2\big]\frac{1}{q^2} - \frac{1}{4}(1+3\eta)\frac{1}{q^3}, \end{aligned} \tag{27}$$

$$\begin{aligned} H_{3PN} = {} & \frac{1}{128}\big(-5 + 35\eta - 70\eta^2 + 35\eta^3\big)\big(\boldsymbol{p}^2\big)^4 \\ & + \frac{1}{16}\big[\big(-7 + 42\eta - 53\eta^2 - 5\eta^3\big)\big(\boldsymbol{p}^2\big)^3 \\ & + (2 - 3\eta)\eta^2(\boldsymbol{n}\cdot\boldsymbol{p})^2\big(\boldsymbol{p}^2\big)^2 \\ & + 3(1-\eta)\eta^2(\boldsymbol{n}\cdot\boldsymbol{p})^4\boldsymbol{p}^2 - 5\eta^3(\boldsymbol{n}\cdot\boldsymbol{p})^6\big]\frac{1}{q} \\ & + \left[\frac{1}{16}\big(-27 + 136\eta + 109\eta^2\big)\big(\boldsymbol{p}^2\big)^2 + \frac{1}{16}(17 \right. \\ & \left. + 30\eta)\eta(\boldsymbol{n}\cdot\boldsymbol{p})^2\boldsymbol{p}^2 + \frac{1}{12}(5 + 43\eta)\eta(\boldsymbol{n}\cdot\boldsymbol{p})^4\right]\frac{1}{q^2} \\ & + \left\{\left[-\frac{25}{8} + \left(\frac{1}{64}\pi^2 - \frac{335}{48}\right)\eta - \frac{23}{8}\eta^2\right]\boldsymbol{p}^2 \right. \\ & \left. + \left(-\frac{85}{16} - \frac{3}{64}\pi^2 - \frac{7}{4}\eta\right)\eta(\boldsymbol{n}\cdot\boldsymbol{p})^2\right\}\frac{1}{q^3} \\ & + \left[\frac{1}{8} + \left(\frac{109}{12} - \frac{21}{32}\pi^2\right)\eta\right]\frac{1}{q^4}. \end{aligned} \tag{28}$$

Note that the Hamiltonian (23) does not depend on the mass of the two bodies but on the mass ratio γ.

Although the three-dimensional system is a complicated, highly non-linear system, this system is typically integrable because four exact integrals of motion exist, which include the conserved energy (23) and the conserved angular momentum vector $\boldsymbol{L} = \boldsymbol{q} \times \boldsymbol{p}$. Therefore, the system is regular and not at all chaotic. In addition, the motion does not precess but is always limited to lying in an invariable plane perpendicular to the initial angular momentum vector. The accuracy of these integrals, such as the energy integral, will be used as a reference indicator for estimating the quality of the Forest–Ruth and Yoshida algorithms according to two distinct Hamiltonian decomposition methods.

3.2.1 *Perturbation decomposition method*

For Eq. (1), we take $H_1(\boldsymbol{p},\boldsymbol{q}) = H_N$ and $H_2(\boldsymbol{p},\boldsymbol{q}) = H_{PN}$. Here, a perturbation decomposition form of the Hamiltonian (23) is used because H_1 is a primary part, but H_2 is a secondary, perturbation part.

H_1 can be calculated by obtaining the analytical solution of the pure Kepler problem and H_2 can be integrated numerically with the second-order implicit midpoint rule (5). Thus, A is exact, but B is not. Throughout this treatment, the above mixed algorithms can be applied to the binary system. We choose the mass ratio $\gamma = 1$, the time step $\tau = 1$, and the initial conditions $(\boldsymbol{p}(0);\boldsymbol{q}(0)) = (0, 0.33, 0; 10.8, 0, 0)$.

Figure 2 shows that the energy error of each algorithm has no secular change with time. This attribute is a basic property of the symplectic integrator. Therefore, the four schemes are symplectic and maintain the energy integral of the system in high accuracy. Some explicit differences exist in the energy errors of these algorithms. The *FR* algorithm and the two Yoshida methods S_4 and S_4^* have almost the same order of accuracy, and the maximum error of the *FR** method is approximately 1000 times larger than that of any of the three algorithms. The accuracy of the method *FR** is nearly equivalent to that of the second-order mixed algorithm S_2^*. Note that the energy error of S_2^* is not plotted in this paper. As a consequence, the numerical proofs completely support the above-mentioned theoretical results.

Let us use the numerical solution of H_1 obtained by using the second-order explicit integrator (4) instead of the analytical solution obtained by using Eq. (3), which means that A is inexact. By repeating the above procedure, we can obtain the energy errors of these algorithms, as shown in Fig. 3. The three methods *FR**, S_4^* and S_4 have results similar to that of Fig. 2. However, the error of *FR* is several orders of magnitude larger in Fig. 3 than in Fig. 2. Figure 3 also shows that *FR** is superior to *FR*. An explicit conflict seems to exist between the numerical and analytical results of both *FR* and *FR** with second-order accuracy. To clarify this doubt, we should note that the *PN* H_2 part is smaller than the Kepler flow H_1 and $\varepsilon \ll 1$ is used to mark the difference between them. The *FR* method remains in the order of A such that the error of *FR* is of order τ^3. By contrast, the error of the *FR** method is in the magnitude of order $\varepsilon\tau^3$ because *FR** and B are of the same order. Thus, the accuracy of *FR** is greatly superior to that of *FR*. *FR** is also close to S_4^* or S_4 because *FR** has an error of order $\varepsilon\tau^3$, but both S_4^* and S_4 hold errors of order τ^5, i.e., the fifth-order error terms of A. If the difference in the magnitude between the two splitting parts H_1 and H_2 is absent, then *FR* and *FR** should have the same-order accuracy. The error of *FR** should be larger than that of each of S_4^* and S_4, as shown in Fig. 1.

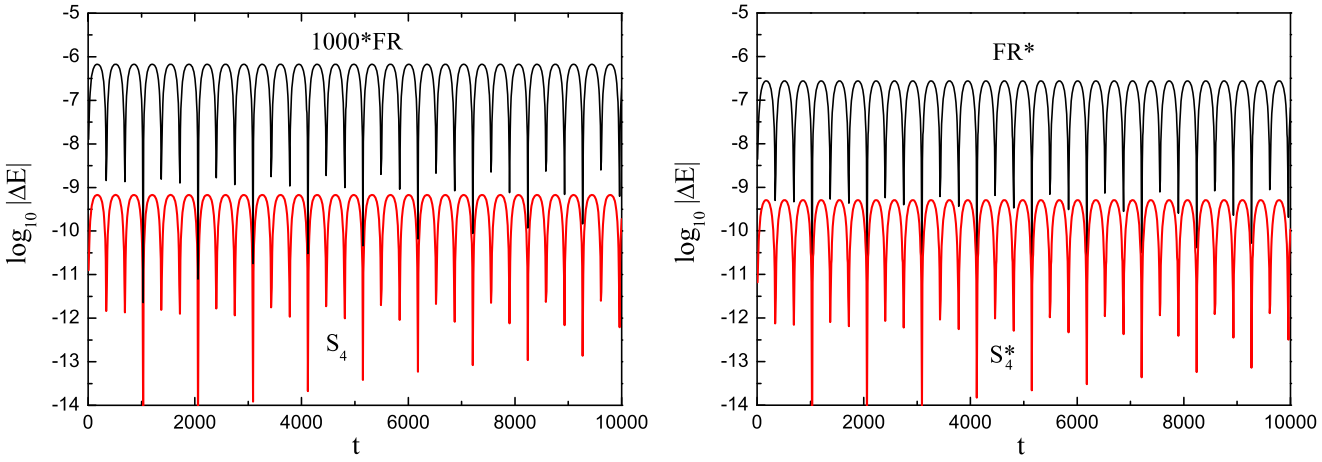

Fig. 2 Energy errors of the Forest–Ruth algorithms *FR* and *FR** and their corresponding Yoshida algorithms S_4 and S_4^* for the *PN* Hamiltonian formulation of non-spinning compact binaries with the perturbation decomposition method. Here, the *Kepler* part H_1 is solved analytically by Eq. (3). The notation $1000 * FR$ denotes that the plotted error ΔE of the method *FR* is 1000 times larger compared with the practical error (Color figure online)

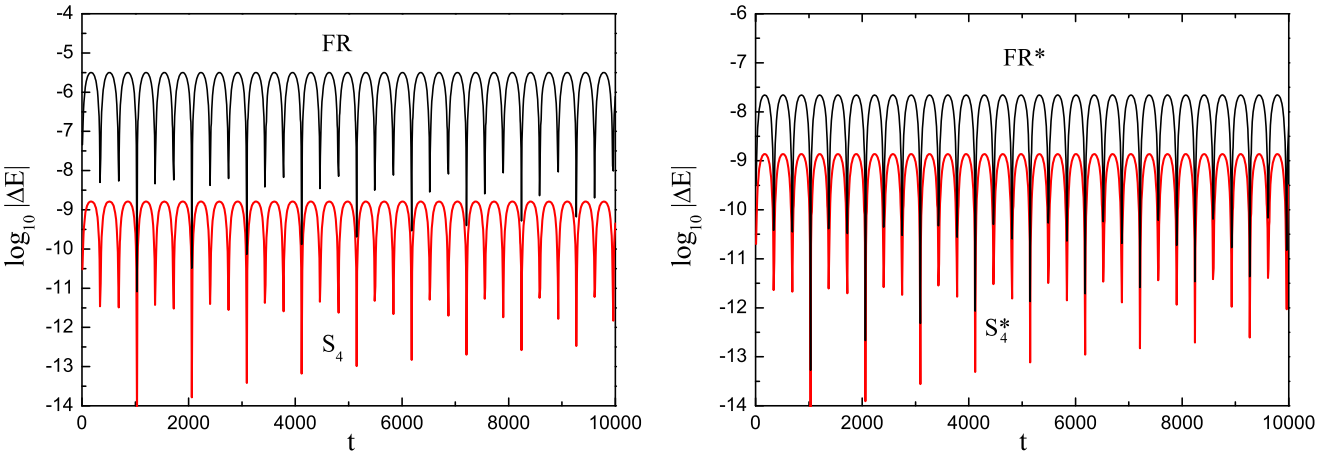

Fig. 3 This figure is the same as Fig. 2, but the *Kepler* part H_1 is solved numerically by the second-order explicit integrator (4) (Color figure online)

Let us confirm the effectiveness of these algorithms when the Hamiltonian (23) consists of a separable variable form of momenta $\boldsymbol{p}$ and positions $\boldsymbol{q}$ and an inseparable variable piece.

3.2.2 *Partial separable variable method*

Unlike the perturbation decomposition method, the partial separable variable method is the Hamiltonian (23) separated into the following parts:

$$H_1 = \frac{1}{8}(3\eta - 1)\big(\boldsymbol{p}^2\big)^2 + \frac{1}{2q^2} + \frac{1}{16}\big(1 - 5\eta + 5\eta^2\big)\big(\boldsymbol{p}^2\big)^3 - \frac{1}{4}(1 + 3\eta)\frac{1}{q^3} + \frac{1}{128}\big(-5 + 35\eta - 70\eta^2 + 35\eta^3\big)\big(\boldsymbol{p}^2\big)^4 + \left[\frac{1}{8} + \left(\frac{109}{12} - \frac{21}{32}\pi^2\right)\eta\right]\frac{1}{q^4} + H_N, \tag{29}$$

$$H_2 = \text{other terms of } H_{PN}. \tag{30}$$

Therefore, all the terms of separable momenta $\boldsymbol{p}$ and positions $\boldsymbol{q}$ are added to the Newtonian term to obtain the H_1 part. The terms associated with inseparable momenta $\boldsymbol{p}$ and positions $\boldsymbol{q}$ are included in the H_2 part. In general, obtaining the analytical solution of H_1 is difficult even if H_1 is integrable. Specifically, the analytical solution of H_1 is nonexistent if H_1 is non-integrable. In this case, numerically calculating H_1 by using the second-order explicit integrator (4) is convenient. The second-order implicit midpoint rule (5) is still used to integrate H_2; i.e., neither A nor B

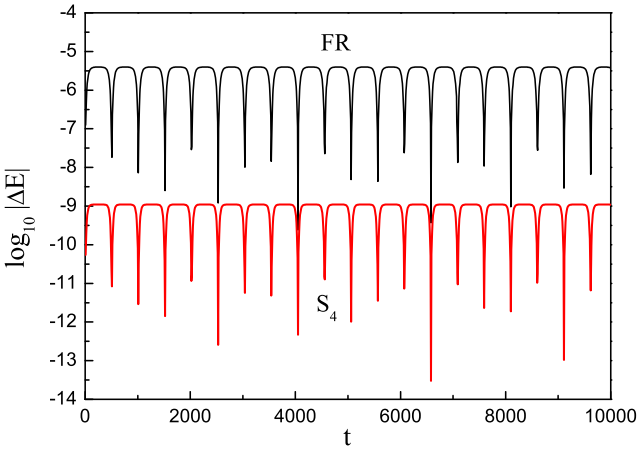

Fig. 4 This figure is the same as Fig. 3, but the *separable variable* part H_1 (29) in the Hamiltonian decomposition method of partial separable variables is solved numerically by the second-order explicit integrator (4) (Color figure online)

is exact. Similar to the demonstration above, the mixed integrators are still applied to solve the Hamiltonian splitting form. The numerical results in Fig. 4, where *FR* and S_4 except FR^* and S_4^* are plotted, are similar to those in Fig. 3. This finding is reasonable because H_2 is smaller than H_1 is for the partial separable variable method such as the perturbation decomposition method. Given that no dramatic difference exists in the accuracy of S_4 between Figs. 4 and 2, the numerical integration in the Hamiltonian decomposition of partial separable variables is worth considering.

For the convenience of readers, we use two tables to conclude the numerical performance of these mixed integrators in Figs. 2–4. Table 1 compares the computational cost of the mixed integrators in all tested cases in terms of CPU times. As expected, S_4^* is the most computationally expensive integrator because this integrator requires six implicit computations of H_2 in each integration step, which in turn require much CPU time. S_4 with *FR* has the highest efficiency because it requires only three computations of H_2. In particular, for the same algorithm S_4, the partial separable variable case is superior to the perturbation decomposition case in terms of computational efficiency because solving the partial separable variable part by using the explicit leapfrog integrator takes less CPU time than solving the Kepler flow by using the analytical method, in which a certain iteration scheme is frequently used to calculate the non-linear Kepler equation. On the basis of this finding, S_4 and the partial separable variable method are worth recommending. Table 2 describes the numerical determination of the order of each mixed symplectic algorithm. A method for numerically determining the order is introduced in this paper. The numerical solution of a numerical method of order K has an accuracy of τ^{K+1} and an energy error of τ^K. When the time step τ is replaced with a new time step $\tau' = \delta \cdot \tau$, the maximum

Table 1 CPU time(s) of each mixed algorithm

Method	*FR*	FR^*	S_4	S_4^*
Fig. 2	6.0	6.5	7.2	9.6
Fig. 3	6.1	6.7	7.4	9.5
Fig. 4	5.8	–	6.9	–

Table 2 Numerical determination of the order K

Case	$\max \lvert\Delta E_\tau\rvert$	$\max \lvert\Delta E_{\tau'}\rvert$	ϱ	K	Method
Fig. 2	6.73e-10	4.23e-11	3.99	4	*FR*
	2.76e-07	6.90e-08	2.00	2	FR^*
	6.73e-10	4.16e-11	4.02	4	S_4
	5.09e-10	3.14e-11	4.01	4	S_4^*
Fig. 3	3.17e-06	7.91e-07	2.01	2	*FR*
	2.20e-08	5.50e-09	2.00	2	FR^*
	1.62e-09	1.01e-10	4.01	4	S_4
	1.37e-09	8.52e-11	4.01	4	S_4^*
Fig. 4	3.97e-06	9.91e-07	2.00	2	*FR*
	–	–	–	–	FR^*
	1.10e-09	6.79e-11	4.02	4	S_4
	–	–	–	–	S_4^*

energy error for the new time step is $(\delta \cdot \tau)^K = \delta^K \cdot \tau^K$, i.e., $\max |\Delta E_{\tau'}| = \delta^K \cdot \max |\Delta E_\tau|$. Thus, we obtain the order K as an integer close to ϱ of the expression

$$\varrho = \log_{(1/\delta)}\big(\max |\Delta E_\tau| / \max |\Delta E_{\tau'}|\big). \tag{31}$$

Without loss of generality, the factor $\delta = 1/2$ is used. Table 2 shows that the algorithms *FR* and FR^* are of second-order accuracy in most cases,[1] but the Yoshida algorithms S_4 and S_4^* are always of fourth-order accuracy in all tested cases. The above results agree with the analytical results in Sect. 2. S_4, S_4^* and *FR* have good accuracy when solving H_1 with the analytical method. In particular, S_4 works well when the Hamiltonian decomposition of partial separable variables is adopted.

4 Summary

This paper provides a detailed discussion of the numerical performance of the Forest–Ruth and Yoshida mixed symplectic methods when some or all of the component integrators are approximate and are second-order with odd-order error structures.

[1] As an exceptional case, *FR* has fourth-order accuracy when H_1 is solved analytically by Eq. (3).

For a Hamiltonian system (1) with two separable and inseparable variable parts, the symmetric compositions of the analytical and numerical solutions can produce second-order mixed symplectic schemes if the separable part is integrable and has an analytical solution and if the inseparable part is solved numerically by the second-order implicit midpoint rule. We can construct the Yoshida algorithms S_4 and S_4^* by using the triple product of the second-order schemes. We can also obtain the Forest–Ruth mixed algorithms *FR* and *FR** by concatenating the edge factors of the Yoshida constructions. From a theoretical point of view, the three integrators *FR*, S_4 and S_4^* are of the same fourth-order accuracy, but the scheme *FR** only has second-order accuracy. In addition, *FR* and S_4 almost have the same computational cost because both of them require three implicit computations of the inseparable variable part in each integration step. By contrast, *FR** and S_4^* do not have the same computational cost because they use four and six implicit computations, respectively. Therefore, *FR* and S_4 have the highest efficiency, and S_4^* has the lowest. The order of magnitude of either *FR* or *FR** becomes 2 and that of either S_4 or S_4^* remains at 4 only when the analytical solution is replaced with the numerical solution through the second-order explicit integrator. Therefore, the accuracy of the Yoshida constructions disagrees with that of the concatenated Forest–Ruth algorithms in this case.

These analytical results can be supported by the numerical simulations of two models, including the *PN* Hamiltonian formulation of non-spin compact binaries. The analytical and numerical results show that the Yoshida constructions have an advantage over the concatenated Forest–Ruth algorithms when the inexact component integrators are used. Moreover, the Yoshida algorithm S_4, which contains three implicit computations of the inseparable variable part, requires less computational cost for the Hamiltonian decomposition of partial separable variables compared with the perturbation Hamiltonian decomposition. Note that the numerical accuracies of the two cases have minimal differences.

To obtain high computational accuracy and efficiency, the *FR* algorithm or the Yoshida algorithm S_4 with a combination of both analytical and implicit numerical solutions should be used in practical computations if the partial separable variable Hamiltonian part is integrable and if the analytical solution is easy to obtain. However, if the partial separable variable Hamiltonian part is integrable but its analytical solution is difficult to solve or if the Hamiltonian part is non-integrable, then the Yoshida algorithm S_4 with a combination of both explicit and implicit numerical solutions should be used. The suggested algorithm and the Hamiltonian decomposition method of partial separable variables will be used in discussing the dynamics of spinning compact binaries [19]. The suggested algorithm will be suitable for treating an N-body *PN* Hamiltonian problem of spinning compact objects [21] because the Newtonian terms in this system, as an N-body Newtonian Hamiltonian problem, is typically non-integrable. Therefore, the proposed algorithm will also be suitable for other partially separable but globally inseparable Hamiltonian problems. In this way, the dynamics of these systems can be described.

Acknowledgements We are very grateful to a referee for true comments and useful suggestions. This research is supported by the Natural Science Foundation of China under Grant Nos. 11173012, 11178002 and 11178014.

References

1. E. Hairer, C. Lubich, G. Wanner, *Geometric Numerical Integration* (Springer, Berlin, 1999)
2. D.Z. Ma, X. Wu, S.Y. Zhong, Astrophys. J. **687**, 1294 (2008)
3. L.J. Mei, X. Wu, F.Y. Liu, Chin. Phys. Lett. **29**, 050201 (2012)
4. G.D. Quinlan, S. Tremaine, Astron. J. **100**, 1964 (1990)
5. R.D. Ruth, IEEE Trans. Nucl. Sci. **30**, 2669 (1983)
6. K. Feng, M.Z. Qin, *Symplectic Geometric Algorithms for Hamiltonian Systems* (Zhejiang Science and Technology Publishing House, Hangzhou China, Springer, New York, 2009)
7. E. Forest, R.D. Ruth, Physica D **43**, 105 (1990)
8. H. Yoshida, Phys. Lett. A **150**, 262 (1990)
9. J. Wisdom, M. Holman, Astron. J. **102**, 1528 (1991)
10. J.E. Chambers, M.A. Murison, Astron. J. **119**, 425 (2000)
11. J. Laskar, P. Robutel, Celest. Mech. Dyn. Astron. **80**, 39 (2001)
12. X.H. Liao, Celest. Mech. Dyn. Astron. **66**, 243 (1997)
13. M. Preto, P. Saha, Astrophys. J. **703**, 1743 (2009)
14. C. Lubich, B. Walther, B. Brügmann, Phys. Rev. D **81**, 104025 (2010)
15. M. Suzuki, Phys. Lett. A **146**, 319 (1990)
16. S.Y. Zhong, X. Wu, S.Q. Liu, X.F. Deng, Phys. Rev. D **82**, 124040 (2010)
17. X. Wu, Y. Xie, Phys. Rev. D **81**, 084045 (2010)
18. I.P. Omelyan, I.M. Mryglod, R. Folk, Comput. Phys. Commun. **146**, 188 (2002)
19. A. Buonanno, Y. Chen, T. Damour, Phys. Rev. D **74**, 104005 (2006)
20. X. Wu, S.Y. Zhong, Gen. Relativ. Gravit. **43**, 2185 (2011)
21. P. Galaviz, Phys. Rev. D **84**, 104038 (2011)